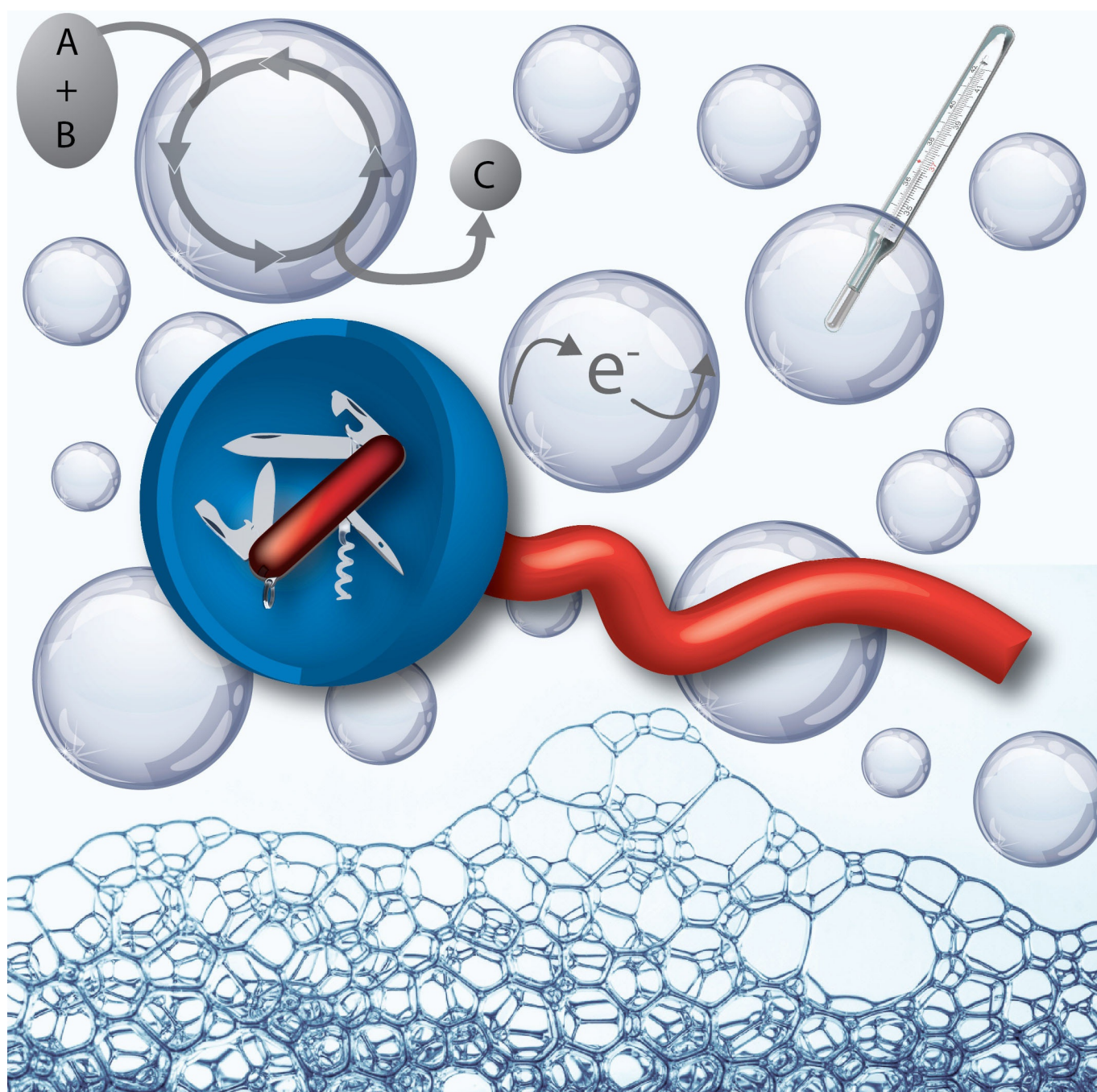


Self-Assembly

## Added-Value Surfactants

Sebastian Polarz,\* Marius Kunkel, Adrian Donner, and Moritz Schlötter<sup>[a]</sup>



**Abstract:** Surfactants are ubiquitous in cellular membranes, detergents or as emulsification agents. Due to their amphiphilic properties, they cannot only mediate between two domains of very different solvent compatibility like water and organic but also show fascinating self-assembly features resulting in micelles, vesicles, or lyotropic liquid crystals. The current review article highlights some approaches towards the next generation surfactants, for example, those with catalytically active heads. Furthermore, it is shown that amphi-

philic properties can be obtained beyond the classical hydrophobic–hydrophilic interplay, for instance with surfactants containing one molecular block with a special shape. Whereas, classical surfactants are static, researchers have become more interested in species that are able to change their properties depending on external triggers. The article discusses examples for surfactants sensitive to chemical (e.g., pH value) or physical triggers (temperature, electric and magnetic fields).

## 1. Introduction

Numerous applications require or at least benefit from an increased interfacial area. However, the existence of surfaces is thermodynamically unfavourable and their creation requires substantial amounts of energy. Surface energy is higher, the more the involved phases differ. Thus, minimization of interfacial energy and maximization of interfacial area can be managed by substances with amphiphilic properties. Those substances are compatible with the two phases and can mediate between them. A special class among amphiphiles are surfactants. The expression “surfactant” is an abbreviation for “surface active agents” indicating their ability for reducing interfacial energy. Anyone encounters surfactants on a daily basis. They occur in any biological organism in the form of phospholipids as a main constituent of the cellular membrane. For instance, the uptake of oxygen from the air would not work so efficiently without pulmonary surfactants present in the lung.<sup>[1]</sup> However, surfactants represent also major industrial products ( $\approx 1.6 \times 10^7$  t per year) with applications in many areas such as detergents, emulsification agents or in phase-transfer catalysis.<sup>[2]</sup> They are also used frequently in nanoscience for stabilization of phases with high surface to volume ratio like nanoparticles or porous materials.

Many systems possess amphiphilic properties including polymers and even certain particles.<sup>[3]</sup> Whereas, there is a certain polydispersity in size, number and distribution of functional groups for the latter, surfactants ideally represent molecular compounds with a precise structure. The hydrophobic moiety, respectively the so-called tail, is typically comprised of a linear alkyl-chain  $[-(\text{CH}_2)_n\text{CH}_3]$ . The chain length can differ, but  $n > 8$  in most cases. However, what distinguishes the different surfactant classes is the nature of their so-called head group,

which is covalently linked to the tail. One major class of surfactants is characterized by a charged head group. This may be a cationic ammonium group such as in CTAB (cetrimonium bromide), but it can also be a heterocyclic unit such as pyridinium or imidazolium, which positions cationic surfactants close to ionic liquids (ILs).<sup>[4]</sup> Heads of anionic surfactants comprise sulfate, sulfonate, phosphate or carboxylate as a functional group. The class of non-ionic surfactants is the largest since their heads can range from ethoxylates to carbohydrates found in glycoside surfactants.<sup>[5]</sup> In each of the mentioned cases, the primary function of the head group is the implementation of compatibility with a polar environment, most importantly water as a solvent. The head can also provide either electrostatic or steric stabilization of colloidal objects dispersed in a continuous phase.

The next level in development are surfactants that have at least one additional property or fulfil one additional task. As the molecular structure of the amphiphilic compounds presented so far is always static, in this article, particular emphasis is put on surfactants, which are able to change their properties initiated by an external trigger (adaptive amphiphiles). The manuscript is organized as follows. For the reader, who is not so familiar with surfactants, a short discussion of their general features will be given in Section 2. Examples for amphiphiles will also be mentioned, which are capable of special modes of self-assembly due to their shape. We will then focus on surfactants with added value. Surfactants with catalytic function will be mentioned in Section 3. How surfactant self-assembly can be influenced by chemical actions or physical triggers will be discussed in Section 4 and 5. The article will be closed by a conclusion and outlook. It is important to note that the current Minireview is not intending to deliver a comprehensive review about all examples published in the literature. We rather selected few, illustrative and important cases to demonstrate current directions in research on the generation of new surfactants.

## 2. Basics of Surfactant Self-Assembly

### 2.1. Conventional surfactants

One of the most impressive properties of amphiphiles is the ability to form so-called association colloids through self-organization of an ensemble of surfactant molecules, when they

[a] Prof. Dr. S. Polarz, M. Kunkel, A. Donner, M. Schlötter  
Department of Chemistry, University of Konstanz  
Universitätsstrasse 10, 78457 Konstanz (Germany)  
E-mail: sebastian.polarz@uni-konstanz.de

 The ORCID identification number(s) for the author(s) of this article can be found under: <https://doi.org/10.1002/chem.201802279>.

 © 2018 The Authors. Published by Wiley-VCH Verlag GmbH & Co. KGaA. This is an open access article under the terms of Creative Commons Attribution NonCommercial License, which permits use, distribution and reproduction in any medium, provided the original work is properly cited and is not used for commercial purposes.

are brought into contact with water. The smallest association colloid is the micelle. Upon increase of the surfactant concentration more and more micelles form. Because the micelles all have the same size, they can eventually pack into higher organized structures with different symmetry, so-called lyotropic liquid crystal phases (LLCs). Further, the micelles can fuse to cylinders adopting a hexagonal arrangement, followed by the formation of lamellar phases.<sup>[6]</sup>

The simplest form of a micelle is a spherical object with approximately twice the diameter of a single surfactant molecule. The surfactants arrange themselves with their heads pointing outwards into the aqueous phase shielding the inner, hydrophobic domain of the micelle. The critical micelle concentration (cmc) is the point, when the first micelles can be observed in solution, at least according to classical theories.<sup>[7]</sup> Prior to reaching the cmc, the air–water interface becomes occupied by surfactant molecules with their tail pointing towards the gas-phase. This process can be monitored by concentration dependent surface tension ( $\gamma$ ) measurements. Surface tension drops quickly until a monolayer of surfactant molecules is reached. The position of the kink on the c-axis of the resulting curve represents the cmc. Using the Gibbs adsorption isotherm, one can also extract the area the surfactant requires at the interface ( $a_e$ ) by calculation of the surface excess.<sup>[8]</sup> The  $a_e$  can also be obtained from application of the Langmuir–Blodgett technique.<sup>[9]</sup> The cmc resulting from these measurements is unfortunately not very precise, which is why alternative analytical methods have been established in the meantime like pulsed field gradient nuclear magnetic resonance, fluorescence spectroscopy, or conductivity measurements.<sup>[10]</sup> Presumably currently the most powerful technique is the isothermal titration calorimetry (ITC).<sup>[11]</sup> In addition to the cmc, one can also gain thermodynamic data ( $\Delta H_{micr}$ ,  $\Delta S_{micr}$ ,  $\Delta G_{mic}$ ) and the aggregation number, which describes how many surfactant molecules are present in one micelle.<sup>[12]</sup>

Spherical micelles are the objects with the highest curvature among alternative geometries. Not every surfactant can adopt such a highly curved structure. The medium curvature ( $\kappa = 1/R_1 + 1/R_2$ ; with  $R_{1,2}$  = radius of curvature of the object) is reduced for rod-like (i.e., worm-like) micelles and becomes 0 for layered aggregates. Lying in between one can find vesicular aggregates.<sup>[6]</sup> Dispersions of anisotropic micelles are highly interesting for instance for the generation of fluids with advanced viscoelastic properties,<sup>[13]</sup> see also the comprehensive article published by Feng et al. in 2013.<sup>[14]</sup> Vesicles are interesting as artificial cells or for drug-delivery applications. Already in 1976 it was Israelachvili,<sup>[15]</sup> who introduced the packing parameter concept for explaining, which surfactant prefers which kind of aggregate, regarding geometrical constraints. The packing parameter  $P$  relates the surfactant tail volume ( $V_0$ ) to the area per molecule at the aggregate interface ( $a_e$ ) and the length of the tail ( $l_0$ ):  $P = V_0 / (a_e \times l_0)$ . Surfactants with a low value of  $P$  ( $< 0.3$ ) look like a cone and, thus, they prefer to adopt highly curved structures (spherical micelles). When the surfactant contains two tails,  $V_0$  increases and ( $a_e \times l_0$ ) remains constant. A surfactant with  $P \approx 1$  has the shape of a cylinder and is expected to form bilayer structures. One can find worm-

like micelles and vesicles for  $P$ -values in between. The advantage of the packing parameter model is its clearness, but the spontaneous formation of aggregates is of course governed by intermolecular interactions and maximization of entropy and, thus, has to be treated by appropriate thermodynamic models.<sup>[16]</sup> Then,  $a_e$  becomes an equilibrium parameter rather than a pure geometric factor, and one can understand much better, why also the length of the hydrophobic tail, the temperature, the salinity of the aqueous phase and the head group charge influence the surfactant behaviour in addition to molecular shape. The self-assembly of surfactants is driven by weak non-covalent forces. It has been learned, that the formation of aggregates in solution is decisively determined by en-

Sebastian Polarz studied chemistry at the University of Bielefeld and received his diploma in 1999 with Prof. A. Müller on polyoxometalate chemistry. He then joined the Max-Planck Institute of Colloids and Interfaces working with Prof. M. Antonietti on confinement effects. After his PhD thesis in 2001, he moved to the group of Prof. G. A. Ozin and conducted research on porous materials. He initiated an Emmy-Noether research group in 2003 in the entourage of Prof. M. Driess first at the Ruhr-University Bochum, then at the Technical University Berlin. Since 2007, he is full professor for "functional inorganic materials" at the University of Konstanz, and his main research interests are on nanoporous organosilica materials, semiconductor nanostructures and new surfactants.



Marius Kunkel (left in picture) studied chemistry at the university of Konstanz and started his PhD in 2017 in the group of Prof. Sebastian Polarz. His research is about novel fullerene-based surfactants, their synthesis, the exploration of their unusual behaviour and their potential application in biological chemistry and material science. Adrian Donner (right) studied chemistry at the University of Konstanz. In 2016, he started his PhD in the group of Prof. Sebastian Polarz. He uses the structural motif of N-heterocyclic carbenes (NHC) as a head group to design new surfactants with incorporated catalytic activity. Moritz Schlötter (centre) studied physics at the University of Konstanz and received his diploma in 2013. He performed his PhD study on light scattering from neuronal tissue in the group of Prof. Georg Maret. In 2017, he joined the group of Prof. Sebastian Polarz to explore the physics of novel surfactants.

tropic factors, which are often summarized as the so-called hydrophobic effect.<sup>[17]</sup> One explanation for the hydrophobic effect is, water molecules have to adopt a special packing in vicinity to the alkyl groups of a monomeric surfactant in solution. Apolar molecules disrupt the hydrogen bonding network in water. This rearrangement of water molecules causes an effective attractive force between hydrophobic substances. At the same time, the alkyl chain cannot adopt the entire conformational freedom. Aggregate formation, like micellization, would then release these water molecules and the tails exist in a random state in the hydrophobic domain, which is entropically favoured. The difference in free energy  $\Delta G$  that accompanies the assembly of one mole of molecules can be linked to the cmc via the approximation<sup>[15a]</sup>  $\Delta G \approx RT \ln(\text{cmc})$ , where  $RT = kTN_A$  is the thermal energy with the Avogadro constant  $N_A$  and the Boltzmann constant  $k$ . A deeper understanding of the aggregation behaviour can be gained by use of the DLVO (Derjaguin, Landau, Verwey, Overbeek) theory of charged colloids. It incorporates van der Waals forces and electrostatic double layer interaction.<sup>[18]</sup> But more detailed descriptions require computational treatment. Here, soft coarse-grained models can simulate more complex systems and predict thermodynamic properties but remain numerically challenging.<sup>[19]</sup>

## 2.2. Non-aqueous systems and shape amphiphiles

All of the latter, classical examples for surfactants rely on the presence of a water-compatible and a hydrophobic molecular entity. An important question is, if compounds (amphiphiles) exist, which show surfactant-like behaviour in non-aqueous solution. Because a major factor for the formation of surfactant aggregates is the hydrophobic effect, as discussed in Section 2.1, it is not obvious what happens, if water is absent.<sup>[20]</sup> Therefore, next, we want to look into non-aqueous solvent systems and other amphiphilic systems with large building blocks in their molecular architecture, so-called shape amphiphiles.

Some noteworthy non-aqueous systems date back to 1960.<sup>[21]</sup> The key factor in those systems is basically the same as for aqueous systems: Combination of solvophilic and solvophobic parts in one molecule.<sup>[22]</sup> The implementation of molecular fragments, which lead to compatibility with a certain organic solvent can easily be achieved. To realize solvophobic properties, it is elemental to integrate functional groups, which exhibit much stronger intermolecular interactions with each other than with the solvent molecules. A possible interaction leading to solvophobic domains is the  $\pi$ - $\pi$  interaction.<sup>[23]</sup> Naphthalene-tetracarboxylic acid diimide (NDI), for instance, is known as constituent in air-stable organic semiconductors.<sup>[24]</sup> The group of Ghosh built up an amphiphilic organic semiconductor based on the NDI core (Figure 1) with adjustable alkyl chain content (solvophilic part).

They could show the formation of liquid crystalline phases in mixtures of chloroform and methylcyclohexane, indicating a wide-range order under distinct conditions.<sup>[25]</sup> The group of Nakanishi et al. used the fullerene  $C_{60}$  as a solvophobic entity, which was modified by "ordinary" hydrophobic groups.<sup>[26]</sup> Upon solvation in *n*-hexane self-assembly takes place as indi-

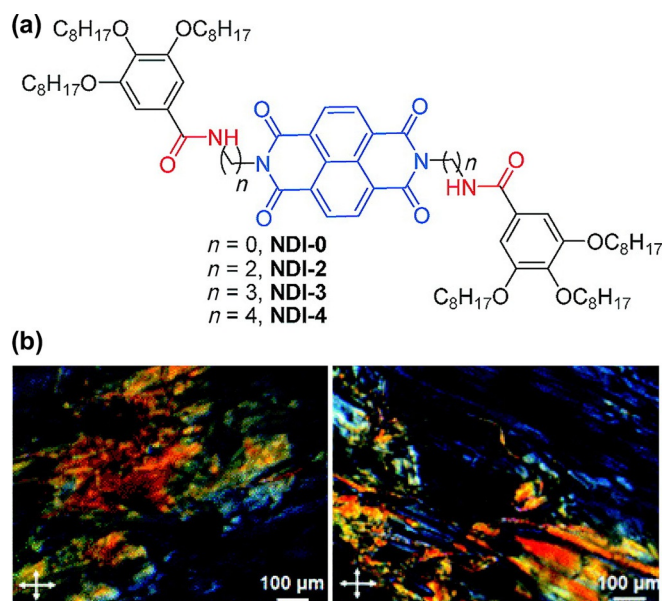


**Figure 1.** Example for amphiphilic self-assembly in the absence of water: LLC-formation (b) of a modified NDI-based chromophore (a) in mixtures of chloroform/methylcyclohexane. Reprinted with permission from ref. [25]; copyright 2011 American Chemical Society.

cated by X-ray methods and cross-polarization microscopy. The tendency of  $C_{60}$  to exhibit  $\pi$ - $\pi$ -interactions is relatively small. Therefore, there must be a different origin for the existence of the solvophobic properties, which leads us to so-called shape amphiphiles.

The defined self-assembly of shape amphiphiles does not anymore derive from an intramolecular difference in polarity. Instead, it is the shape effect that leads to self-assembly, specifically the rigidity in molecular shape. Thus, shape amphiphiles contain different building blocks, whose packing geometries are incompatible with each other. During self-assembly these building blocks prefer not to mix, but separated domains form, and this leads to hierarchical structure formation. The shape effect was proposed by Date et al. after experimenting with phase-separating mixtures of molecular disks and rods.<sup>[27]</sup> They found the presence of a compound containing a disc-like building block and a rod-like building block in one molecule prevents the phase separation. To enable not miscible systems to mix is obviously one key property of amphiphiles. In the following, substantial work was investigated to explore the self-assembly of shape amphiphiles in more detail. Common structural concepts for the formation of shape amphiphiles are the combination of rod-like parts with disc-like building blocks, most commonly aromatic molecules like coronene, isocrysene or star-like phenyl derivatives.<sup>[28]</sup> A study on the formation of superstructures by a disc-bent-core shape amphiphiles was presented by Gu et al.<sup>[29]</sup> They linked a bent-core (BC) molecule with an internal angle of  $120^\circ$  to a discotic hexa-peri-hexabenzocoronene (HBC) (Figure 2). HBC is known for forming columnar phases and BC causes structural asymmetry. The authors observed the formation of spiral superstructures, and a mechanism in three steps was proposed. The  $\pi$ - $\pi$  interaction of the HBC building block first leads to the formation of a columnar

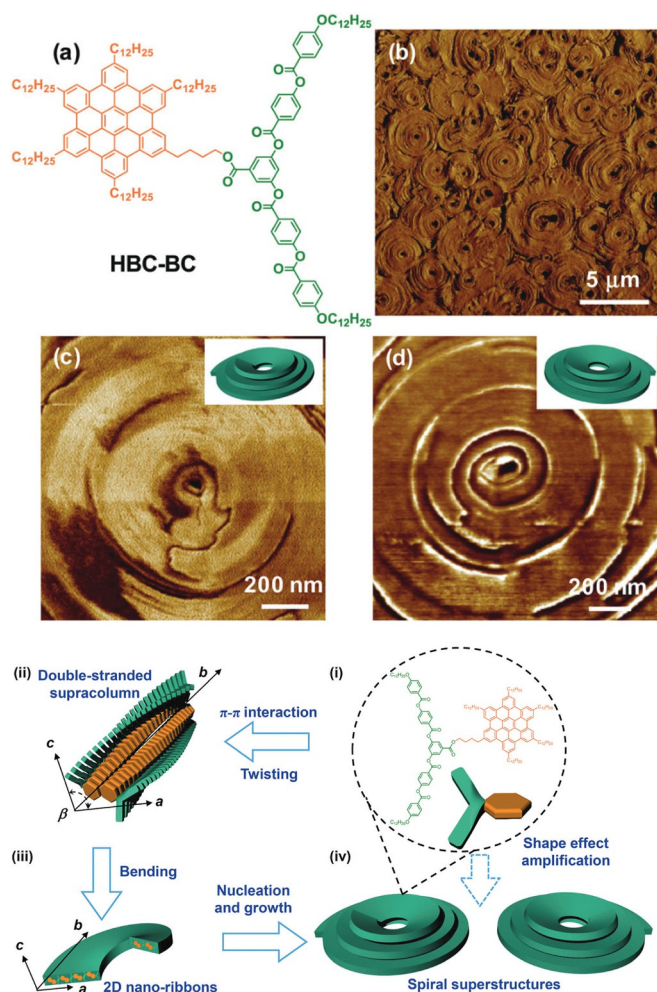


**Figure 2.** Molecular structure and appearance of aggregates formed by a disc-bent core shape amphiphile presented by Gu et al. and formation mechanism of spiral superstructures.<sup>[29]</sup> Reprinted with permission from ref. [29]; copyright 2017 The Royal Society of Chemistry.

structure, and further to a twisted double-stranded supracolumn induced by the asymmetry of the molecule. The resulting asymmetric steric hindrance leads to bending, which is then responsible for the formation of 2D nanoribbons (Figure 2). Nucleation and growth of the latter let the spiral superstructures appear.

More exotic building blocks used in shape amphiphiles involve spheres and cubes, which can be combined with rods or discs. Several combinations for fullerene shape amphiphiles are known in literature, like sphere-rod,<sup>[30]</sup> sphere-square/disc<sup>[31]</sup> or even sphere-cube<sup>[32]</sup> combinations. As a cubic building block, polyhedral oligomeric silsequioxane (POSS) is commonly used.<sup>[33]</sup> One can also combine the mentioned heads of a shape amphiphile with highly flexible tails. An example was presented by Yu et al. in 2012.<sup>[30c]</sup> A special hydrophilic fullerene derivative was linked to one or two polystyrene (PS) chains with different length. The authors demonstrate the occurrence of self-assembled structures like spherical micelles or vesicles in concentration dependent experiments. This change in morphology results from the structural change due to

longer chains. The morphology is directly related to the cross-section of the C<sub>60</sub> head group and PS tails. An example for a cube-rod shape amphiphile based on POSS and its properties was given by Cheng and co-workers.<sup>[33d]</sup> A giant surfactant consisting of a polar POSS head group and a PS tail was prepared, and the authors documented the self-assembly process into different micellar morphologies. PS-APOSS can form vesicles, wormlike structures, and spheres in solution. These changes can be induced by changing the headgroups degree of ionization. The authors argue, that the PS chains are highly stretched, in contrast to conventional block copolymers such as PS-*b*-PAA.

### 3. Catalytic Surfactants

Converting two reactants with different solvent compatibility, one hydrophilic and the other lipophilic, is a classic problem in chemistry. This problem can be overcome by two different methods. One method is widely known as phase-transfer catalysis,<sup>[34]</sup> in which one component is moved into the unfavourable phase by coordination to auxiliaries changing its solubility. Another method is to increase the chance for a reaction by providing a large interface of the immiscible phases. This can be done by creating micelles or emulsion droplets. The current state in the associated field "micellar catalysis" was described in excellent review articles from Scarso et al. in 2015 and Lipshutz et al. in 2018.<sup>[35]</sup> The situation becomes even more intricate as soon as the catalysts itself is not soluble in the desired medium. Many molecular catalysts are soluble in apolar solvents due to bulky, organic ligands coordinating to the metal. The application of those compounds in polar media, ultimately water, requires extra effort. Here, we recommend the review published by Bhattacharya in 2009.<sup>[36]</sup> However, a remaining challenge is the compatibility of the catalytically active species with two solvents of opposing miscibility at the same time. Therefore, it would be desirable, if the surfactant itself plays a more active role during catalysis.

One possibility, which has been used already for quite some time, is the application of surfactants with a chiral head in enantioselective catalysis.<sup>[37]</sup> The surfactant interacts more or less directly with the catalytic species and influences the stereochemistry of the reaction.<sup>[38]</sup> Chaudret and co-workers used an amphiphile containing a chiral oxazoline head group.<sup>[39]</sup> These molecules could interact with the surfaces of Ru<sup>0</sup>-nanoparticles. The hybrid material was then active in an enantioselective hydrogenation reaction of carbonyl groups. Yamanaka et al. attached a chiral BINOL (binaphthol) derivative to phosphoric acid as a soluble moiety and showed impressive results for the enantioselective Mannich reaction.

However, the development of surfactant-combined catalyst, which are catalytically active by themselves, stands at its beginning. Mingotaud and co-workers have presented a Hoveyda's type catalyst comprising a perfluorinated C<sub>9</sub>-chain attached to Ru via a carboxylate group in 2008.<sup>[40]</sup> Some impressive examples exist on pincer complexes with amphiphilic design used for C-C cross-coupling reaction. For instance, Uozumi et al. prepared Palladium-NCN pincer complexes with

one side modified by two alkyl chains as hydrophobic moieties and (on the other side) two oligo glycol chains for water solubility (see Figure 3). In several publications, the authors show that the product selectivity in the Miyaura–Michael reaction can be improved in comparison to using conventional, non-amphiphilic catalysts.<sup>[41]</sup> Our group has recently presented a surfactant containing an *N*-heterocyclic carbene (NHC) head.<sup>[42]</sup> The coordination to Pd led to a system that was able to catalyse Suzuki coupling reactions much faster than a non-amphiphilic reference system.

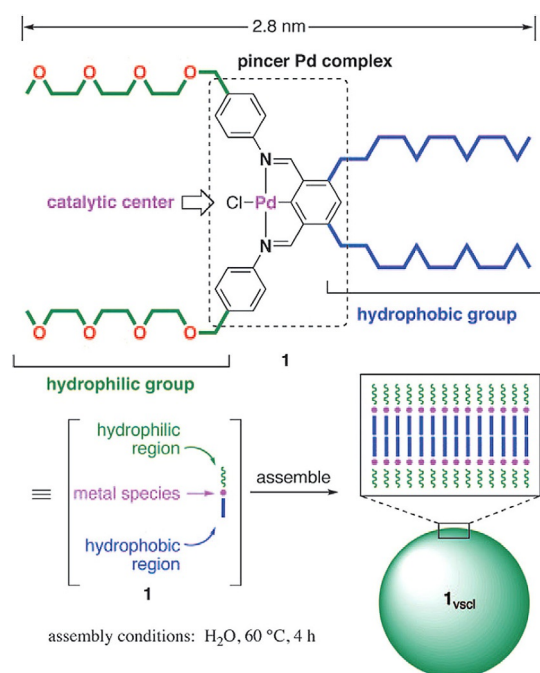


**Figure 3.** Molecular structure and self-assembly of the Pd-pincer amphiphile used for the catalytic Miyaura–Michael reaction. Reproduced from with permission ref. [41a]; copyright 2011 Wiley-VCH.

## 4. Changing the Packing Parameter by Chemical Triggers

### 4.1. pH-sensitive surfactants

In Section 1, we discussed that three molecular adjustments are possible for altering the packing parameter: The length of the hydrophobic chain, the extension, and the charge of the head group. The variation of the surfactant length is quite easy to achieve, because one can transfer the synthesis of a particular system and perform it with a series of analogous alkyl-compounds. A change in the character of the head group is much more fundamental, since it will have a major impact on the entire chemistry of the surfactant. In case one wants to investigate the effect of the head group charge, one should ideally exclude a modification of the molecular shape of the surfactant at the same time. This condition is obviously violated, when one introduces more than one charged group to the surfactant, finally ending up in a head group with polyelectrolyte design.<sup>[43]</sup> A proton ( $H^+$ ) is, as opposed to the latter, such a

small entity, it would barely change the architecture of the surfactant. Consequently, several researchers have looked into the effect, when the head group charge changes due to protonation/deprotonation processes. These surfactants are also known as pH-responsive surfactants.<sup>[44]</sup> Amines are the most obvious choice for Brønsted bases implemented into the molecular structure of the amphiphile. A good example was published by Eastoe and co-workers,<sup>[45]</sup> who are among the pioneers in the field of stimuli-responsive surfactants. Because the head contained a diaminopropane moiety with two different  $pK_a$  values associated to the primary and secondary amine, the protonation degree and charge differs depending on pH value. The presence of two functional groups in the head group is special, and is called bola(form) architecture, a common feature for pH-sensitive amphiphiles. Both groups are protonated at low pH values, and spherical aggregates with high curvature form because of the maximum value for  $a_e$ . If the pH value is raised, the charge is reduced continuously, and the authors could observe a transition to worm-like micelles and eventually vesicles (see Figure 4).<sup>[45]</sup>

The described concept can be extended to other systems. For instance, Wang et al. presented a pH-sensitive amphiphile containing the imidazolium group showing a micelle to vesicle transition as well.<sup>[46]</sup> Because the mentioned processes lead to a significant change of the volume confined inside the self-assembled structure, there is a possible application as drug-deliv-

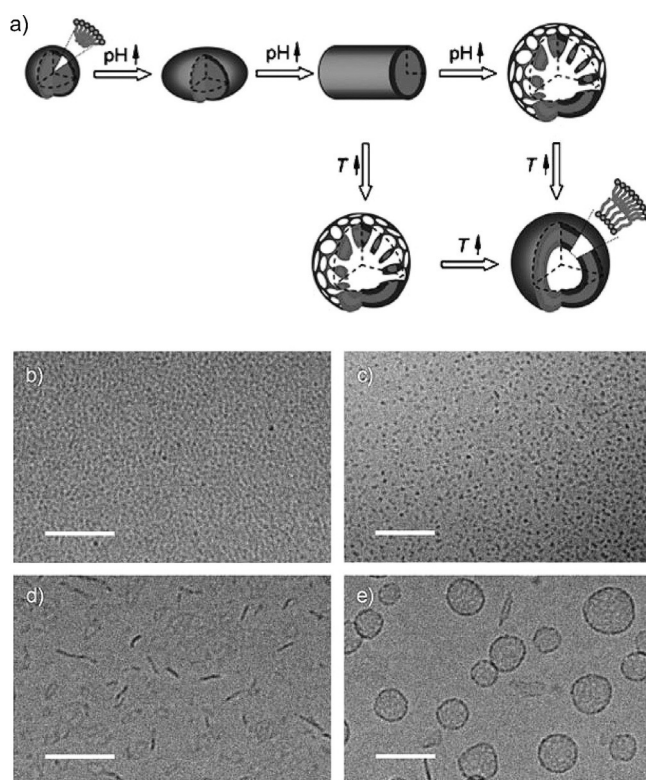


**Figure 4.** pH value dependent self-assembly of the surfactant *N*-dodecyl-1,3-diaminopropane showing the transition in aggregate shape from spherical micelles to rod-like micelles and vesicles. Schematic representation (a) and TEM images (b, c, d, e). Reprinted with permission from ref. [45]; copyright 2010 Wiley.

ery systems.<sup>[47]</sup> It is known, that infected or cancerous tissue has a lower pH than under normal physiological conditions. If a shape transition takes place exactly in this pH-window, one could trigger the local release with a desired pharmaceutical. The mentioned topic is also related to pH-responsive molecular capsules, for example, presented by the Yoshizawa group.<sup>[48]</sup>

One can also find reports in the literature about CO<sub>2</sub>-responsive amphiphiles. An early, prominent case described by Jessop and co-workers involves compounds modified with amidine groups.<sup>[49]</sup> In analogy to carbon capture systems, one could think of a direct reaction of CO<sub>2</sub> with the amines. However, this not the case. The infiltration of water with CO<sub>2</sub> leads to a drop in pH-value, and then the surfactant head group becomes protonated. Therefore, the mechanism is very similar to the pH-sensitive surfactants described above. An advantage is, the process is highly reversible, and often it is sufficient to purge an inert gas like N<sub>2</sub> or argon through the solution. Thus, this additional property of a surfactant can be used for the reversible aggregation and de-aggregation of colloidal particles.<sup>[50]</sup>

A single protonation of the head group would obviously not lead to a highly charged system. As described before, the synthesis of compounds with higher charges requires the introduction of more groups, and as a result the charge would also be distributed in a larger volume. Polarz and co-workers could establish a different way by facilitating polyoxometalates as functional heads of anionic surfactants.<sup>[51]</sup> Figure 5 shows such a surfactant.

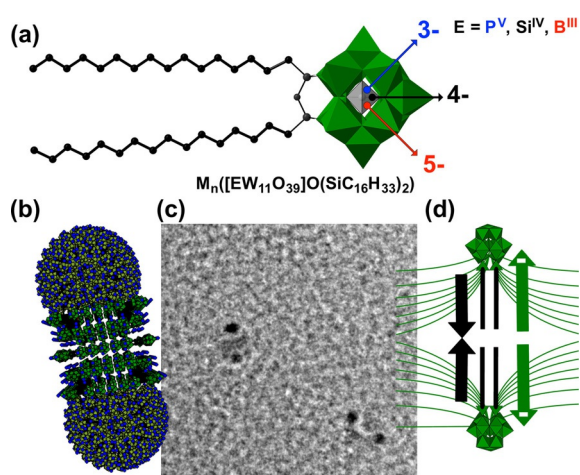


**Figure 5.** Variation of the head group charge without changing the surfactant shape.<sup>[52]</sup> (a) Structure and composition of the POM-based surfactants. Unusual bipolar micelles observed for highly charged compounds, Scheme (b) and TEM image (c). Model for interaction responsible for the unusual structuration processes (d).

One of the special features is that the central element of the polytungstate oxocluster can be varied, and this results in a different charge (3<sup>-</sup> → 4<sup>-</sup> → 5<sup>-</sup>).<sup>[52]</sup> It is obvious that the geometric structure of the head remains the same. It was obvious that the self-assembled structures formed by the triply charged surfactant are still common for amphiphiles in general like spheri-

cal micelles and hexagonal LLCs. A head with a negative charge of 4 leads to significant deviations. The micelles (Figure 5b,c) have a different shape with a dipolar character. Only irregular structures were found, after going to charge of 5<sup>-</sup>, which indicated that the self-assembly processes are now hampered. A possible explanation could be, that into the direction of the hydrophobic domains of the self-assembled structures (Figure 5d) there is no effective shielding of the electric field created by the head's charge. An increasing charge will then result in enhanced electrostatic repulsion adding to the "normal" attractive forces responsible for aggregate formation.

#### 4.2. Redox-modulated surfactant self-assembly

Reversible switching of the charge via the manipulation of the oxidation state of a functional group is realized by incorporation of a redox-responsive unit into amphiphiles. Common used examples are ferrocene (Fc), disulfide (-S-S-) and diselenide (-Se-Se-) moieties.<sup>[53]</sup> Another building block used for the preparation of redox-active surfactants is anthraquinone.<sup>[54]</sup> They can be divided into two types: Moieties which remain bonded to the amphiphile (Fc) and groups which are cleaved upon stimulation (disulfide, diselenide). Upon oxidation of a ferrocene unit, the iron(II) centre is transformed into iron(III) resulting in a positive charge. Disulfide and diselenide bonds are broken up upon reduction leaving two separate molecules (Figure 6). These transformations can lead to interesting changes in the resulting self-assembled structures of the surfactant solution due to changes in polarity or molecular structure, respectively.

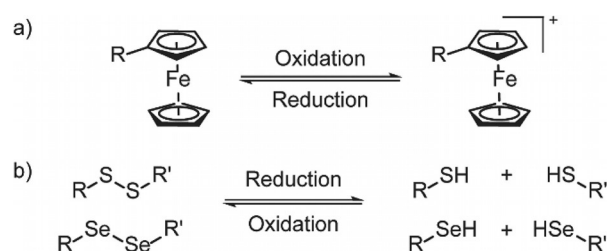


**Figure 6.** (a) Oxidation and reduction of the ferrocene (Fc) unit and (b) Cleavage of disulfide and diselenide moieties upon reduction.

Many redox-active surfactants are based on the pioneering work of Saji et al., who reported their first results on ferrocene-based systems already in 1985.<sup>[55]</sup> Since then, numerous papers have been published, showing that surfactant features are influenced by oxidation leading to ferrocenium (charge +1), such as cmc, minimal surface tension  $\gamma_{\min}$  or aggregate structure.<sup>[56]</sup> A good summary about ferrocene-based surfactants was given by Abbott et al.<sup>[57]</sup> That ferrocene is still a valuable building block for redox-active surfactants is demonstrated in a work by Fan et al. published in 2017. The group developed a surfactant system which carries a cyclodextrin structure covalently linked to a ferrocene unit via alkyl-linkers with different lengths (Figure 7).<sup>[53]</sup> They were able to examine various intramolecular complexation modes of the ferrocene terminus

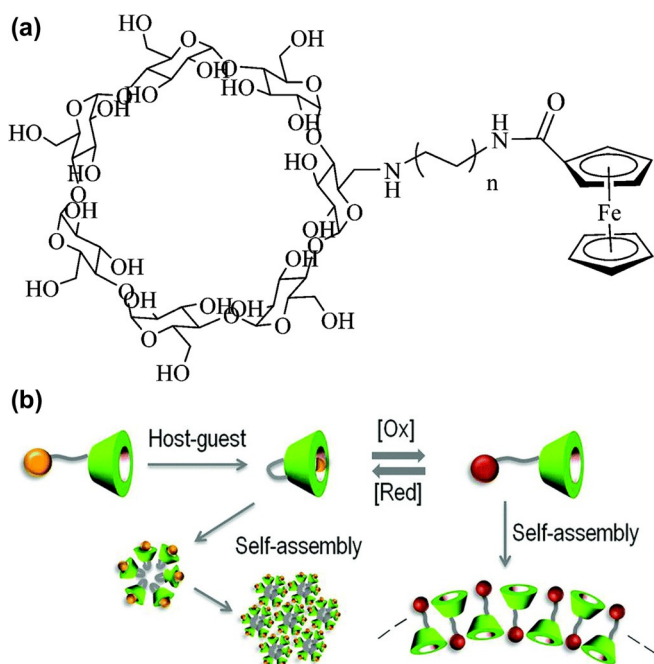


**Figure 7.** Cyclodextrin/ferrocene based surfactant (a) and oxidation state dependent self-assembly (b). Reproduced with permission from ref. [53]; copyright (2017) Royal Society of Chemistry.

inside the cyclodextrin cavity, depending on the length of the alkyl chain. Oxidation of the ferrocene unit revealed a dramatic change in surfactant behaviour due to the decomplexation of the ferrocene. This behaviour enables the use of these compounds for controlled molecule uptake and release, for example, for drug delivery.

The group of Pei et al. used the redox-active properties of ferrocene together with the structural motif of pillararenes to obtain a switchable bola-amphiphile.<sup>[58]</sup> This system showed the formation of bilayer vesicles upon the oxidation by  $\text{FeCl}_3$ , capable of taking up an exemplary drug (doxorubicin hydrochloride) together with the drug resistance gene silencing siRNA, whereas the reduction by natural abundant glutathione (GSH) led to the destruction of the vesicles, thus releasing the drug mixture in the living cell. Polymeric surfactants, like polyalkyleneglycol ethers, may also be equipped with redox-switchable moieties. Several examples for ferrocene-containing monomers are known, whose polymer products show switchable self-assembly behaviour.<sup>[59]</sup>

As already mentioned, disulfide and diselenide moieties are another group of redox sensitive functions. Zhang et al. presented an amphiphile based on hyaluronic acid which is covalently bound to deoxycholic acid via a disulfide bridge.<sup>[60]</sup> They could show the formation of micellar structures with high storage capacities of the cancer drug paclitaxel (PTX). Again, GSH triggered the dissolution of the micelles and release of the drug. For the sake of completeness, the class of selenium containing surfactants should be mentioned, although they are not attracting much attention due to their high toxicity.<sup>[61]</sup> However, the groups of Zhang and Liu synthesized two such

selenium-surfactants and studied their self-assembling behaviour upon oxidation.<sup>[62]</sup>

The previously described class of surfactants with polyoxometalate heads is also redox-active.<sup>[51a,63]</sup> The oxidation state of W or Mo can be changed reversibly from VI to V, and as a result the head group charge can be varied.<sup>[64]</sup> In 2012, Polarz and co-workers presented a system, which allowed to change the charge of the head group stepwise from  $-1$ ,  $-2$ ,  $-3$  to  $-4$  and backwards via electrochemistry, and effects on the size and shape of micellar aggregates were documented.<sup>[64]</sup> Because the electron(s) in a reduced polyoxometalate cluster is at least partially delocalized, the group became then interested in the generation of a conductive surfactant. This was achieved by attaching a  $\pi$ -conjugated tail instead of the electrically insulating alkyl groups.<sup>[65]</sup> It could be proven that charge carriers can move from the polyoxometalate head to the chain and backwards leading to semiconductor properties or applications as micellar batteries.

## 5. Influencing Surfactant Self-Assembly by Physical Triggers

From the previous paragraph, one can see that advanced surfactants are able to react on various chemical triggers. A disadvantage of these approaches is, the stimuli-response processes are relatively slow, and the composition of the entire system is likely to be changed. The advantages of pure physical triggers are, the chance for complete reversibility is higher, because the composition of the system remains constant and they may be applied much more rapidly.

### 5.1. Temperature-adaptive systems

Temperature is the simplest physical parameter, which can be adapted very easily. The  $T$ -dependency of phases belongs to the first information scientists have gathered about surfactants, and the data is recorded in phase diagrams. In general, temperature has a crucial effect on the solubility of the amphiphiles. The solubility of ionic surfactants increases with higher temperature with soaring at the so-called Krafft temperature ( $T_K$ ).<sup>[66]</sup> Micellization takes place above  $T_K$ , and below surfactant monomers tend to separate into macrophases. The effect can be opposite for non-ionic surfactants, because their solubility strongly depends on hydrogen bonding to the water molecules. Because the hydrogen bonds are weakened at higher temperature, the solubility of the amphiphiles may decrease.<sup>[67]</sup> Therefore, a certain  $T$ -sensitivity is intrinsic to any amphiphile, it is not special. However, surfactant systems exist, which have been designed to react in a much more direct way to changes in temperature.

The mentioned type of amphiphiles contain a special thermo-responsive block, which is often combined with a hydrophilic block. The thermosensitive part can be switched from a hydrophobic to a hydrophilic state. It is clear, that such a change has significant effects on the amphiphilic properties. The most prominent example of a molecular structures with the desired properties is poly(*N*-isopropylacrylamide)

(PNIPAM).<sup>[68]</sup> Below the lower critical solution temperature (LCST) these compounds are highly soluble in water. When heated above the LCST, the molecular structure gets dehydrated and the respective part of the amphiphile becomes insoluble. In combination with a hydrophilic block this process induces a phase separation and leads to surfactant-like self-assembly.<sup>[69]</sup> An intriguing example can be taken from the paper published by Pietsch et al. in 2012 (see Figure 8).<sup>[69e]</sup>

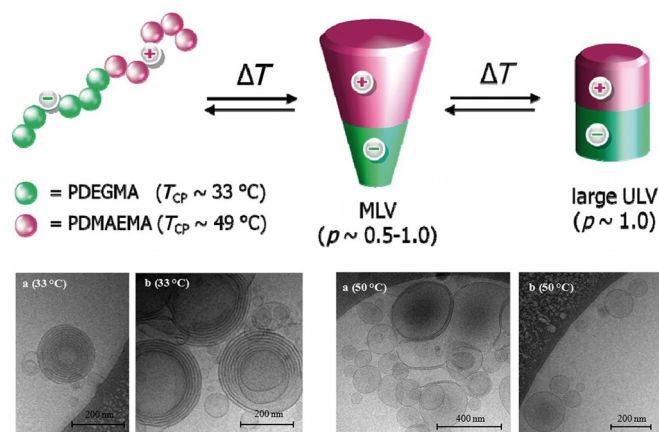


**Figure 8.** The double thermoresponsive di-block amphiphile and its aggregates formed above LCST 1 and LCST 2. Reprinted with permission from ref. [69e]; copyright (2012) American Chemical Society.

The special aspect of the work by Pietsch et al. is that not only one block of the amphiphile is thermoresponsive, but both, resulting in two LCSTs.<sup>[69e]</sup> After the first LCST at 33 °C, the compound assembled into multilamellar vesicles and above the second LCST at 50 °C. into unilamellar vesicles. The intramolecular ionic interaction is the driving force for this special behaviour. The negatively charged block becomes insoluble at the first LCST. The positively charged block, which is still soluble at this temperature, leads to a layer-by-layer assembly to vesicles with a multi-layer, onion-like architecture. If the temperature is increased further, also the solubility of the second block decreases, so does the overall hydrophobicity of the amphiphile. This consequence is a change in hydrophilic to hydrophobic cross-section and the transition to unilamellar vesicles (Figure 8). An amphiphile was presented by Weiss et al., which exhibits triple temperature sensitivity.<sup>[69b]</sup> A series of poly(*N*-*n*-propylacrylamide) (PNPAM, A), poly(methoxydiethylene glycol acrylate) (PMDEGA, B), and poly(*N*-ethylacrylamide) (PNEAM, C) triblock copolymers of different combinations (ABC, BAC and ACB) have been investigated. Since every single block has a different LCST the system can be varied from pure hydrophilic to amphiphilic with the hydrophobic constituents in different segments. Then, the self-assembly properties crucially depend on the order of the blocks.

A different system using a thermos-responsive building block is the molecular dumbbell shaped rod amphiphile investigated by Kim et al.<sup>[70]</sup> It consists of a conjugated rod segment that is grafted by hydrophilic polyether dendrons at one end and hydrophobic branches at the other end. In solution this

compound forms micrometer sized spherical aggregates with a porous shell (Figure 9). Upon heating to 65 °C the compound's aggregates lose their porosity and form a closed shell without any changes in spherical shape. The pores slowly started to reopen for cooling to room temperature. This gating behaviour of the pores was explained by the oligo(ethylene oxide) dendritic segment which becomes less hydrophilic above the LCST. The hydrodynamic volume of the segment decreases, forming a closed structure with flat interfaces.

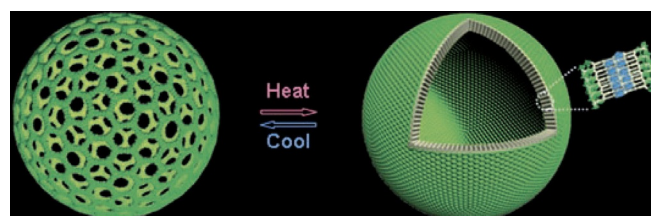


**Figure 9.** Thermo-induced opening and closing of capsules formed by self-assembly of a stimuli-responsive amphiphile. Reprinted with permission from ref. [70]; copyright (2008) Wiley-VCH.

## 5.2. Light-adaptive systems

The desire for the creation of molecular motors has driven an enormous development in photoswitches.<sup>[71]</sup> These special, molecular entities are able to react with a reversible and very defined change of conformation when irradiated with a certain wavelength. Azobenzene derivatives are the classical example. The treatment with UV-light induces a *trans*→*cis* transformation. This induces an angle into the structure of the entire molecule, the dipole moment and eventually also the hydrophilic-hydrophobic balance change.<sup>[72]</sup> The possibility to modify different systems with either azobenzene, stilbene or fluorenes paved the way towards the use of photoswitches in different areas of material chemistry.<sup>[44,57,73]</sup> The application of photoswitches in surfactant science was pioneered by Shinkai et al.,<sup>[74]</sup> who presented a compound containing azobenzene. The authors could only demonstrate an indirect evidence for the modification of the amphiphilic properties by exposure to light. However, other researchers who used azobenzene-containing systems showed clearly that all key surfactant properties can be modified using photosensitive surfactants.<sup>[72,75]</sup> The extent of the possible changes were demonstrated by Hartley and co-workers published in 2014.<sup>[76]</sup> The authors performed photorheological measurements (Figure 10). The drastic change in viscosity of the dispersion was caused by a photo-induced transition from an LLC-state to a micellar state.

Another highly interesting approach was presented by Zhang and co-workers in 2007 on a surfactant containing azobenzene and pyridinium as a cationic head forming a rotaxane with  $\alpha$ -cyclodextrin as a second, hydrophilic group.<sup>[77]</sup> The *cis*-conformer could not anymore form an inclusion complex with the cyclodextrin. Thus, the photochemical process induced the relocation of the cyclodextrin, which changed the self-assembly properties of the surfactant significantly. Azobenzenes as photoswitches have several disadvantages. For instance, the

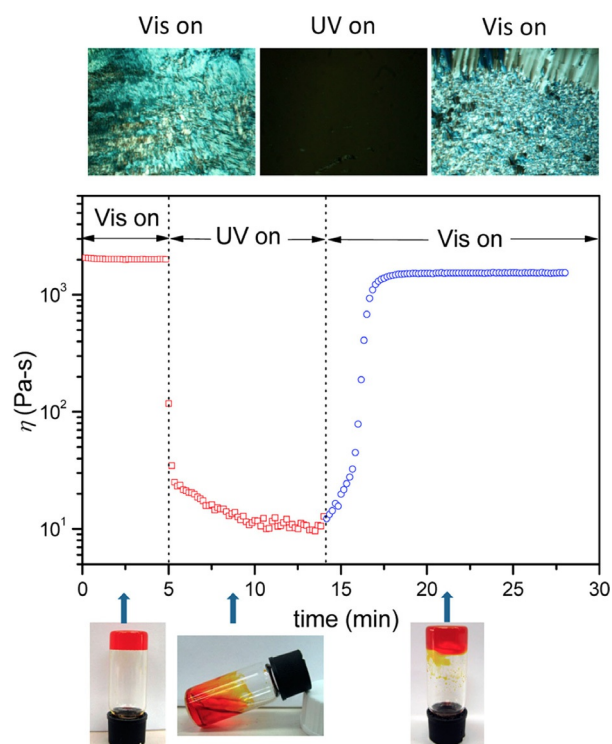


**Figure 10.** Optical polarized microscopy images, photographs and in situ rheological measurements showing the LLC→micelle transition on an azobenzene-containing surfactant triggered by light radiation. Reproduced with permission from ref. [76]; copyright (2014) American Chemical Society.

conversion efficiency is never 100% and also the backreaction is triggered by thermal energy. These disadvantages are absent for other photoswitches like spiropryrane moieties. Several researchers could successfully synthesize the respective surfactants.<sup>[78]</sup>

An entirely different approach was selected by Fameau and co-workers in 2015.<sup>[79]</sup> The authors have used the pH-sensitive properties described above (see Section 4.1). Instead of the integration of a photoswitch into the molecular structure of the surfactant, a photoacid generator (diphenyliodonium nitrate) was present in solution. The irradiation of the photogenerator leads to a change of the pH-value, and this induced protonation of the surfactant and the structural aggregate changes associated with the modification of the packing parameter.

### 5.3 Electric-field response

Because surfactant aggregates are typically observed in water it is questionable, if the application of an electric field ( $E$ ) makes sense. The polarity of the solvent molecules and also the presence of solvated ions are responsible for an effective shielding against an external  $E$ . In fact, there are no reports describing the deformation or phase-transition of micelles. However, the situation is different for emulsion droplets or vesicles.<sup>[80]</sup> The shape of vesicles is not static, but thermally undulated due to the softness of the bilayer. In the absence of external fields, the shape fluctuates around a global minimum of the bending energy. Giant unilamellar vesicles provide a novel

model system to study the interaction of self-assembled structures with external fields. A variety of phenomena can be observed including deformation, poration, fusion and finally bursting. This particular subject was covered in previous reviews.<sup>[81]</sup> The aim of this section is to give a brief introduction to the involved phenomena and its consequences. When the vesicle is approximated as a thin spherical dielectric layer, a homogeneous external field will pile up charges along the membrane. In a static field, the vesicle gets charged similar to a capacitor. Its transmembrane voltage is described by Equation (1):

$$V_m = \frac{3}{2}ER\cos\theta \left[ 1 - \exp\left(\frac{-t}{\tau_c}\right) \right] \quad (1)$$

The transmembrane voltage is at its maximum where the membrane is perpendicular to the electric field ( $\theta = 0^\circ$  and  $\theta = 180^\circ$ ). Here  $E$  is the external field,  $R$  the vesicle radius and the charging time  $\tau_c$  is given by Equation (2):

$$\tau_c = \frac{RC_m}{\sigma_{in}} \left( 1 + \frac{\sigma_{in}}{2\sigma_{ex}} \right) \quad (2)$$

with internal and external conductivities  $\sigma_{in,ex}$  and membrane capacity  $C_m$ . In aqueous systems where  $\sigma_{in,ex} \approx 1\mu S/cmR = 10\mu m$  and vesicles with  $R_0$  exhibit charging timescales  $\tau_c \approx 1ms$ .<sup>[82]</sup> However, above a critical voltage  $V_c$ , the membrane gets destabilized and pores appear. At even higher fields, the membrane will eventually collapse completely. Typical membranes form pores around 1 V, and the critical external field is around  $70 Vmm^{-1}$  [from Eq. (1)]. This is a very rough estimation since the critical values strongly depend on the lipid phase,<sup>[83]</sup> lipid head and tail architecture and membrane asymmetry.<sup>[84]</sup> The destabilization can be utilized to fuse vesicles with each other or with biological cells.<sup>[85]</sup> Destabilization of the membrane is furthermore a promising candidate for advanced drug delivery. Though many aspects like biocompatibility or biological barrier crossing remain challenging.<sup>[86]</sup>

External electric fields induce ion currents in the internal and external medium. The timescale for mobile charges to respond to the external field is given by the Maxwell Wagner time  $\tau_{MW} = \epsilon/\sigma \approx 10^{-5} s^{-1}$ , where  $\epsilon$  is the permittivity and  $\sigma$  the conductivity of the medium. Since the membrane is impermeable to those charges, the vesicle experiences a mechanical stress, but morphological response of the membrane is retarded by the viscosity  $\mu_{in,ex}$ . The time it takes to deform is given by Equation (3):

$$\tau_d = \frac{\mu_{ex}}{\epsilon_0\epsilon_e E^2} \left( 1 + \frac{\mu_{in}}{\mu_{ex}} \right) \quad (3)$$

Small electric fields cause an entropic flattening, where the thermal fluctuations of the membrane are diminished. At higher fields, the stress stretches the membrane and increases its area. When a dc field is switched on, the vesicle undergoes a charging phase where the electrolyte kinetics inside and outside of the membrane determine the deformation. After charg-

ing, an equilibrium state is reached, where the field is expelled from the inside of the vesicle. This final state causes a prolate deformation (see Figure 11 c). In the charging phase, the shape is dictated by the ratio between internal and external conductivity [Eq. (4)].

$$\chi = \frac{\sigma_{in}}{\sigma_{ex}} \quad (4)$$

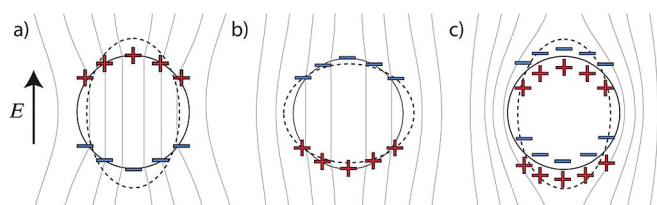


**Figure 11.** Charging dynamics and deformation of vesicles in a constant electric field. (a)  $t < \tau_c$  and  $\chi > 1$ ; (b)  $t < \tau_c$  and  $\chi < 1$ ; and (c)  $t \gg \tau_c$ . The subsequent deformation is displayed with the dashed lines. Reproduced with permission from ref.[82]; copyright (2014) Royal Society of Chemistry.

Charges pile up on the inside first when  $\chi > 1$  and produce a prolate ellipsoid (see Figure 11 a). In the opposite case the model suggests that an oblate shape may be observed, as long as  $\tau_{ed} < t < \tau_c$  (see Figure 11 b).<sup>[87]</sup> This condition is difficult to fulfil because higher external fields are required, that are likely to induce poration.

However, a high field can be applied for a short time without introducing pores, as long as the membrane potential does not reach the critical value [see Eq. (2)]. The oblate-prolate transition can be observed using a two-step pulse, where a short pulse produces the oblate shape, while avoiding poration. A second sub-critical pulse drives the relaxation into a prolate shape.<sup>[82]</sup> The simplified theory explains the ellipsoidal shape transformations well, but with increasing ion concentration strange cylindrical shapes have been observed.<sup>[88]</sup> The squaring is short-lived and happens between the prolate-oblate transitions (see Figure 12). Simulations could reproduce this phenomenon. Additionally, they predicted bistable configurations, where the vesicle oscillates between the prolate and oblate shape.<sup>[89]</sup>

Alternating (ac) electric fields provide an experimentally simpler access to the regime where the shape depends on the conductivity ratio  $\chi$ . At low frequencies, where  $f \ll \tau_c^{-1}$ , the shape is prolate, as expected from the behaviour in dc fields. A

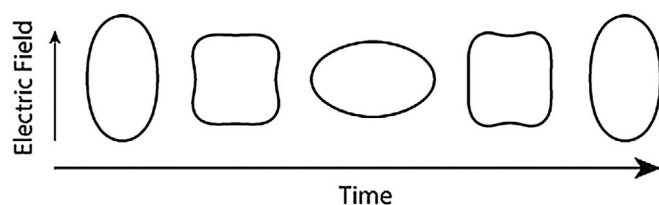


**Figure 12.** Squaring of vesicles in presence of ions. Between the prolate-oblate transitions, short-lived cylindrical shapes can show up. Reproduced with permission from ref.[89]; copyright (2015) Royal Society of Chemistry.

continuous ac field with  $f \gg \tau_c^{-1}$  keeps the system in a stationary non-equilibrium state. If also  $f < \tau_d^{-1}$  (see eq. 1) the stress deforms the vesicle and the oblate shape appears (see Figure 13).

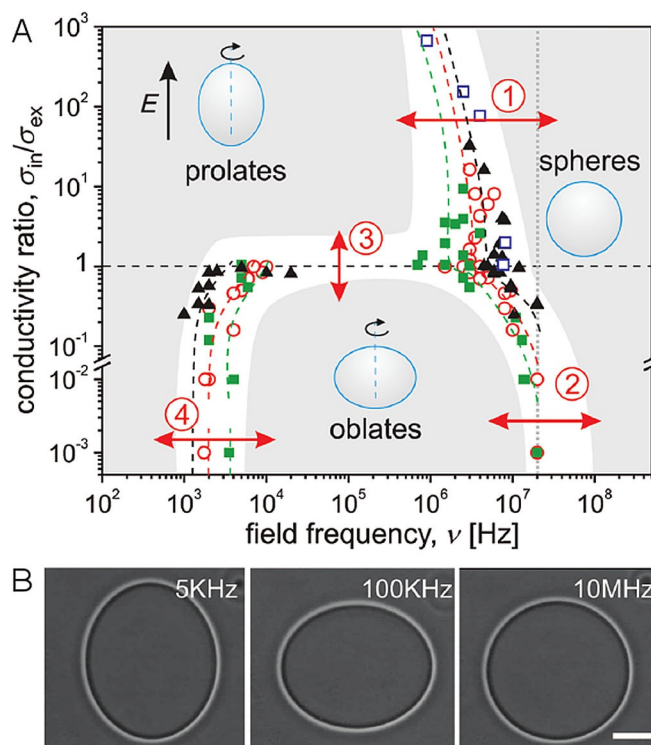


**Figure 13.** Morphology diagram of vesicles in ac fields with a magnitude of  $0.2\text{ kV/cm}$ . The conductivity ratio  $\chi = \sigma_{in}/\sigma_{ex}$  is denoted on the vertical axis and the ac field frequency on the horizontal axis. Four distinct shape transitions can be identified (1–4). (B) Example of images achieved by phase-contrast microscopy at  $\chi = 0.5$ , the scale bar is  $10\mu\text{m}$ . Reproduced with permission from ref. [90]; copyright (2010) American Chemical Society.

The investigation of new morphologies is limited by electroporation. There are a couple of possible factors where functional surfactants could overcome these limitations. The first order theory, as provided, tells us that increasing membrane thickness  $h$  or permittivity  $\epsilon_m$  will extend the non-equilibrium phase (from Eq. 2 and  $C_m = \epsilon_m h$ ). Probably more important is the non-linear effect of lipid architecture, where specifically designed surfactants could expand the experimentally accessible regime, to discover new physics.

#### 5.4. Magneto-adaptive systems

Electric fields, which have been discussed before, are strongly shielded in an aqueous electrolyte. This is not the case for magnetic forces, because water and most salts are diamagnetic. Therefore, it would be highly interesting to equip surfactants with magneto-responsive properties. It is obvious, that a necessity for a magnetic surfactant is persistent unpaired electrons have to be present. The magnetic moment can either be provided by an organic compound (less common) or a paramagnetic metal ion.

Most paramagnetic organic compounds are very reactive because of their open electronic structure. This high reactivity makes them not very suitable as surfactants aimed for an application in aqueous solvent systems. However, one can find examples for persistent and highly stable, organic radicals in the area of electron paramagnetic resonance (ESR) spin-probes.<sup>[91]</sup> Most important are organic nitroxides like the TEMPO (tetramethylpiperidinyloxidanyl) moiety, which is also used for catalytic oxidation reactions and in polymerization chemistry.<sup>[92]</sup> An example for the implementation of TEMPO into an amphiphilic structure was published in 2007 by Saito and co-workers.<sup>[92]</sup> The sulfonic-acid derivative of TEMPO was the counter-ion to the imidazolium-based amphiphile bound together by electrostatic forces. The approach to just mix the surfactant with the magnetic constituent is by far dominant in the field of magnetic amphiphiles.<sup>[93]</sup> This is also true for surfactant systems containing magnetic metal cations. A representative case is  $\text{FeCl}_3$  added to the afore mentioned imidazolium-based amphiphiles, resulting in the formation of the new, paramagnetic  $[\text{FeCl}_4]^-$  counterion.<sup>[94]</sup> A force acting on those anions created by an external magnetic field, will also have an impact on the entire surfactant system, because cation and anion are electrostatically bound to each other.<sup>[95]</sup> Because the paramagnetic centre is free in rotation, the magnetic field cannot create a torque in the latter cases. Therefore, it would be highly interesting to determine the magnetic ion as an integral part of the surfactant by covalent linkage. The most suitable approach to achieve this is the generation of a ligand as a pre-surfactant species, which then becomes the magnetic amphiphile after coordination to the metal cation. Our group presented an example based on a DOTA (tetraxetan) based system (see Figure 14).<sup>[96]</sup>

DOTA is a chelating ligand capable of binding to various metal cations, and it can be modified with exactly one hydrocarbon chain of different length (Figure 14a). Metal cations like  $M^{2+}$  ( $M = \text{Mn}, \text{Co}, \text{Ni}, \text{etc.}$ ) are bound in an octahedral fashion (Figure 14b). One carboxyl group is remaining free, which means the surfactant is actually mono-anionic regarding its overall charge. Several interesting features have been observed. Although the packing parameter of all shown surfactants is the same, the magnetic moment had an influence on the minimum surface tension and also the size of the micellar aggregates (Figure 14c). These are clear indications, that an additional magnetic interaction is present between the surfactant molecules. The behaviour of the surfactants has also been influenced by external, magnetic fields. The minimum surface tension can for instance be lowered, when the field is applied. With approximately 1 T the necessary field strength was low and is technically available. We could also show, there is an effect on the micellization behaviour. The micelles are spherical at  $B=0$  T. However, when the field is turned on, a transition to elongated micelles takes place. Amphiphiles possessing an even higher magnetic moment can be prepared via the reaction with  $\text{Dy}^{3+}$ .<sup>[96a]</sup> The amphiphiles undergo a very unusual, hierarchical self-assembly process, which ends up in particles at macroscopic dimensions (Figure 14d). Although the surfactant is still paramagnetic, one observes macroscopic magnetization

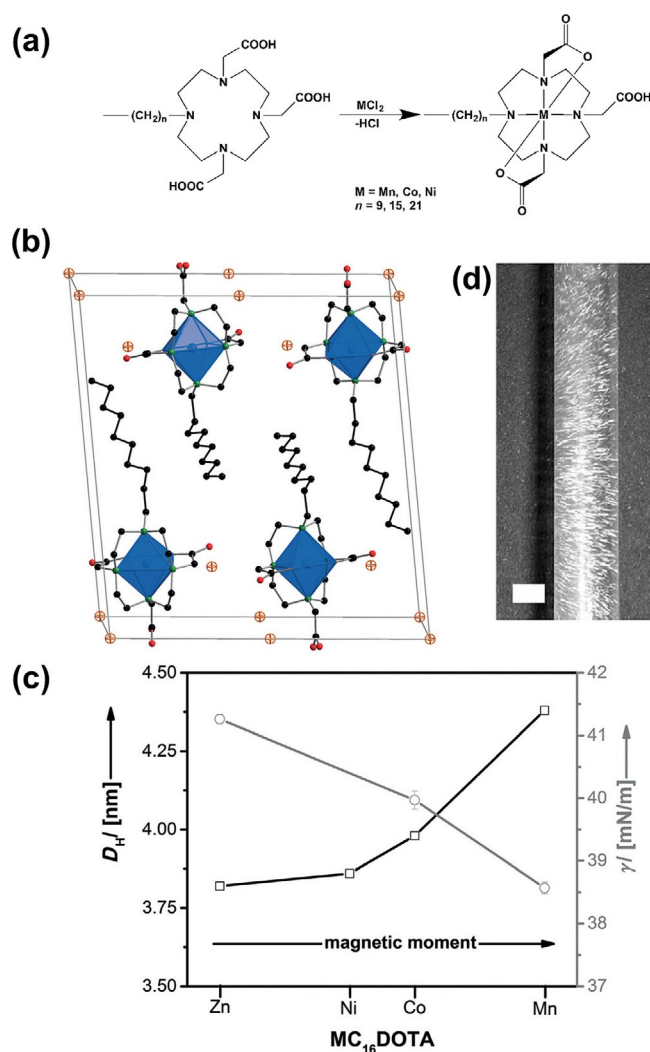


**Figure 14.** (a) Synthesis of DOTA-based, magnetic surfactants.<sup>[96b]</sup> (b) Structure of the surfactant after metal cation ( $M^{2+}$ ) coordination. (c) Influence of the head's magnetic moment on surface tension and micellar aggregate size. (d) Aggregates formed by a surfactant containing  $\text{Dy}^{3+}$  oriented in a magnetic field.<sup>[96a]</sup>

phenomena. The particles readily orient themselves inside an external magnetic field (1 T). The latter experiment underlines the importance of magnetic anisotropy created by the anisotropy of the self-assembled surfactant structure.

## 6. Conclusions and Outlook

The current article has highlighted some of the current developments in surfactant science. Successful efforts to reach beyond the classical domain of amphiphiles have been shown. Surfactants are becoming multifunctional compounds, which are capable of much more than just stabilize interfaces or self-assemble into micelles or vesicles. The systems are inspired from existing, non-amphiphilic compounds and their functionality, which are then integrated as a constituent into the amphiphile, often as the head group. These systems need to overcome two very general problems. Since a surfactant always has

a dipolar character, it is necessary to find a way for an asymmetric modification of the non-amphiphilic paragon, for example, the attachment of one hydrocarbon chain. Second, the introduction of large organic groups is likely to increase the hydrophobicity of the compound. At least, for an application in water, one has then to take additional actions for enhancing the hydrophilic character to compensate for this. Considering these arguments, one can say, first and foremost, synthetic efforts are pivotal for the generation of next generation surfactants.

Several examples were given, how the set of properties were supplemented by an additional functionality like catalytic activity, or stimuli-responsive properties. It could be seen that the self-assembly character of amphiphiles enhances the chances for cooperative effects. This means the new system exhibits some properties (e.g., field-dependent surface tension) neither of the single constituents has. Besides the optimization of surfactants for technologies they are already used in, this can be seen as a large opportunity for establishing new areas in the future. Despite the fact one can now alter the properties of surfactants by external triggers and intervene, one is still ignoring the dynamic aspects. Can we use stimuli-responsive surfactants to learn something about self-organization and structure formation at non-equilibrium conditions?

## Acknowledgements

The work of the authors is funded by an ERC consolidator grant (I-SURF; project 614606).

## Conflict of interest

The authors declare no conflict of interest.

**Keywords:** magnetic surfactants · metallosurfactants · self-assembly · shape amphiphiles · surfactant-combined catalysts

- [1] J. Pérez-Gil, *Biochim. Biophys. Acta Biomembr.* **2008**, *1778*, 1676–1695.
- [2] a) S. D. Naik, L. K. Doraiswamy, *Aiche J.* **1998**, *44*, 612–646; b) D. Albanese, *Mini-Rev. Org. Chem.* **2006**, *3*, 195–217; c) K. Holmberg, *Curr. Opin. Colloid Interface Sci.* **2003**, *8*, 187–196.
- [3] a) S. Förster, M. Antonietti, *Adv. Mater.* **1998**, *10*, 195; b) D. M. Vriezema, M. C. Aragones, J. Elemans, J. Cornelissen, A. E. Rowan, R. J. M. Nolte, *Chem. Rev.* **2005**, *105*, 1445–1489.
- [4] J. P. Hallett, T. Welton, *Chem. Rev.* **2011**, *111*, 3508–3576.
- [5] a) I. F. Uchegbu, S. P. Vyas, *Int. J. Pharm.* **1998**, *172*, 33–70; b) W. von Rybinski, *Curr. Opin. Colloid Interface Sci.* **1996**, *1*, 587–597.
- [6] H. Hoffmann, *Adv. Mater.* **1994**, *6*, 116–129.
- [7] L. D. Song, M. J. Rosen, *Langmuir* **1996**, *12*, 1149–1153.
- [8] H. Yunfei, S. Yazhou, L. Honglai, L. Dominique, S. Anniina, *Langmuir* **2012**, *28*, 3146–3151.
- [9] D. Kabir-ud-Din, G. Sharma, A. Z. Naqvi, *Colloids Surf. A* **2011**, *385*, 63–71.
- [10] a) U. R. M. Kjellin, J. Reimer, P. Hansson, *J. Colloid Interface Sci.* **2003**, *262*, 506–515; b) B. Dong, N. Li, L. Q. Zheng, L. Yu, T. Inoue, *Langmuir* **2007**, *23*, 4178–4182; c) J. F. Yan, M. B. Palmer, *J. Colloid Interface Sci.* **1969**, *30*, 177–182.
- [11] a) D. J. F. Taylor, R. K. Thomas, J. Penfold, *Adv. Colloid Interface Sci.* **2007**, *132*, 69–110; b) K. Bouchemal, F. Agnely, A. Koffi, M. Djabourov, G. Ponchel, *J. Mol. Recognit.* **2009**, *23*, 335–342.
- [12] a) P. Garidel, A. Hildebrand, R. Neubert, A. Blume, *Langmuir* **2000**, *16*, 5267–5275; b) N. E. Olesen, P. Westh, R. Holm, *J. Colloid Interface Sci.* **2015**, *453*, 79–89.
- [13] a) C. A. Dreiss, *Soft Matter* **2007**, *3*, 956–970; b) J. Yang, *Curr. Opin. Colloid Interface Sci.* **2002**, *7*, 276–281; c) D. P. Acharya, H. Kunieda, *Adv. Colloid Interface Sci.* **2006**, *123*, 401–413.
- [14] Z. L. Chu, C. A. Dreiss, Y. J. Feng, *Chem. Soc. Rev.* **2013**, *42*, 7174–7203.
- [15] a) J. N. Israelachvili, *Intermolecular and Surface Forces*, 3rd ed., Elsevier, San Diego, **2011**, pp. 1–674; b) J. N. Israelachvili, D. J. Mitchell, B. W. Ninham, *J. Chem. Soc. Faraday Trans.* **1976**, *72*, 1525–1568.
- [16] a) C. Tanford, *J. Phys. Chem.* **1974**, *78*, 2469–2479; b) C. Tanford, *Proc. Natl. Acad. Sci. USA* **1974**, *71*, 1811–1815; c) R. Nagarajan, *Langmuir* **2002**, *18*, 31–38.
- [17] a) P. Alexandridis, J. F. Holzwarth, T. A. Hatton, *Macromolecules* **1994**, *27*, 2414–2425; b) E. E. Meyer, K. J. Rosenberg, J. Israelachvili, *Proc. Natl. Acad. Sci. USA* **2006**, *103*, 15739–15746.
- [18] D. Lombardo, M. A. Kiselev, S. Magazù, P. Calandra, *Adv. Condens. Matter Phys.* **2015**, *2015*, 151683.
- [19] M. Müller, *J. Stat. Phys.* **2011**, *145*, 967–1016.
- [20] M. Facchin, A. Scarso, M. Selva, A. Perosa, P. Rielo, *RSC Adv.* **2017**, *7*, 15337–15341.
- [21] a) D. Chandler, *Nature* **2005**, *437*, 640; b) N. Pilpel, *Trans. Faraday Soc.* **1961**, *57*, 1426–1433; c) A. Ray, *J. Am. Chem. Soc.* **1969**, *91*, 6511–6512; d) P. Debye, W. Prins, *J. Coll. Sci.* **1958**, *13*, 86–98.
- [22] Y.-W. Zhong, Y. Matsuo, E. Nakamura, *J. Am. Chem. Soc.* **2007**, *129*, 3052–3053.
- [23] F. D'Souza, O. Ito, *Chem. Commun.* **2009**, 4913–4928.
- [24] H. E. Katz, A. J. Lovinger, J. Johnson, C. Kloc, T. Siegrist, W. Li, Y. Y. Lin, A. Dodabalapur, *Nature* **2000**, *404*, 478.
- [25] M. R. Molla, S. Ghosh, *Chem. Mater.* **2011**, *23*, 95–105.
- [26] M. J. Hollamby, M. Karny, P. H. H. Bomans, N. A. J. M. Sommerdijk, A. Saeki, S. Seki, H. Minamikawa, I. Grillo, B. R. Pauw, P. Brown, J. Eastoe, H. Möhwald, T. Nakanishi, *Nat. Chem.* **2014**, *6*, 690.
- [27] R. W. Date, D. W. Bruce, *J. Am. Chem. Soc.* **2003**, *125*, 9012–9013.
- [28] a) P. H. Kouwer, G. H. Mehl, *Angew. Chem. Int. Ed.* **2003**, *42*, 6015–6018; *Angew. Chem.* **2003**, *115*, 6197–6200; b) P. H. Kouwer, G. H. Mehl, *J. Mater. Chem.* **2009**, *19*, 1564–1575; c) P. H. Kouwer, J. Pourzand, G. H. Mehl, *Chem. Commun.* **2004**, 66–67.
- [29] K. Gu, T. Wen, M. Han, W. Zhang, Z. Zhang, Y. Zhou, Z. Shen, X. Fan, R.-M. Ho, *Chem. Commun.* **2017**, *53*, 11794–11797.
- [30] a) F.-a. Teng, F.-l. Liu, L. Han, Z.-j. Zhu, Y.-f. Zhang, Z.-j. Wu, Z.-w. Han, W.-b. Zhang, H. Li, *Chin. J. Polym. Sci.* **2017**, *35*, 503–514; b) F. A. Teng, Y. Cao, Y. J. Qi, M. Huang, Z. W. Han, S. Z. Cheng, W. B. Zhang, H. Li, *Chem. Asian J.* **2013**, *8*, 1223–1231; c) X. Yu, W.-B. Zhang, K. Yue, X. Li, H. Liu, Y. Xin, C.-L. Wang, C. Wesdemiotis, S. Z. Cheng, *J. Am. Chem. Soc.* **2012**, *134*, 7780–7787; d) K. S. Kumar, A. Patnaik, *Langmuir* **2011**, *27*, 11017–11025.
- [31] a) C. L. Wang, W. B. Zhang, X. Yu, K. Yue, H. J. Sun, C. H. Hsu, C. S. Hsu, J. Joseph, D. A. Modarelli, S. Z. Cheng, *Chem. Asian J.* **2013**, *8*, 947–955; b) W.-W. Liang, C.-F. Huang, K.-Y. Wu, S.-L. Wu, S.-T. Chang, Y.-J. Cheng, C.-L. Wang, *Chem. Sci.* **2016**, *7*, 2768–2774.
- [32] a) H.-J. Sun, Y. Tu, C.-L. Wang, R. M. Van Horn, C.-C. Tsai, M. J. Graham, B. Sun, B. Lotz, W.-B. Zhang, S. Z. Cheng, *J. Mater. Chem.* **2011**, *21*, 14240–14247; b) F. Yang, C. Li, H. Guo, J. Ye, Z. Jiao, *Synth. Commun.* **2012**, *42*, 3664–3669.
- [33] a) J. He, K. Yue, Y. Liu, X. Yu, P. Ni, K. A. Cavicchi, R. P. Quirk, E.-Q. Chen, S. Z. Cheng, W.-B. Zhang, *Polym. Chem.* **2012**, *3*, 2112–2120; b) K. Yue, C. Liu, K. Guo, K. Wu, X.-H. Dong, H. Liu, M. Huang, C. Wesdemiotis, S. Z. Cheng, W.-B. Zhang, *Polym. Chem.* **2013**, *4*, 1056–1067; c) Z. Wang, Y. Li, X.-H. Dong, X. Yu, K. Guo, H. Su, K. Yue, C. Wesdemiotis, S. Z. Cheng, W.-B. Zhang, *Chem. Sci.* **2013**, *4*, 1345–1352; d) X. Yu, S. Zhong, X. Li, Y. Tu, S. Yang, R. M. Van Horn, C. Ni, D. J. Pochan, R. P. Quirk, C. Wesdemiotis, *J. Am. Chem. Soc.* **2010**, *132*, 16741–16744; e) K. Yue, C. Liu, K. Guo, X. Yu, M. Huang, Y. Li, C. Wesdemiotis, S. Z. Cheng, W.-B. Zhang, *Macromolecules* **2012**, *45*, 8126–8134.
- [34] a) C. M. Starks, *J. Am. Chem. Soc.* **1971**, *93*, 195; b) T. Ooi, K. Maruoka, *Angew. Chem. Int. Ed.* **2007**, *46*, 4222–4266; *Angew. Chem.* **2007**, *119*, 4300–4345.
- [35] a) G. La Sorella, G. Strukul, A. Scarso, *Green Chem.* **2015**, *17*, 644–683; b) H. Lipshutz Bruce, S. Ghorai, M. Cortes-Clerget, *Chem. Eur. J.* **2018**, *24*, 6672–6695.

- [36] S. Bhattacharya, N. Kumari, *Coord. Chem. Rev.* **2009**, *253*, 2133–2149.
- [37] a) T. Akiyama, *Chem. Rev.* **2007**, *107*, 5744–5758; b) S. Kobayashi, K. Manabe, *Acc. Chem. Res.* **2002**, *35*, 209–217; c) B. H. Lipshutz, S. Ghorai, *Org. Lett.* **2012**, *14*, 422–425.
- [38] a) C. F. Pan, Z. Y. Wang, *Coord. Chem. Rev.* **2008**, *252*, 736–750; b) Z. C. Lin, J. H. Li, Q. F. Huang, Q. W. Wang, L. Tang, D. Y. Gong, J. Yang, J. Zhu, J. G. Deng, *J. Org. Chem.* **2015**, *80*, 4419–4429.
- [39] S. Jansat, D. Picurelli, K. Pelzer, K. Philippot, M. Gomez, G. Muller, P. Lécante, B. Chaudret, *New J. Chem.* **2006**, *30*, 115–122.
- [40] A.-F. Mingotaud, M. Krämer, C. Mingotaud, *J. Mol. Catal. A* **2007**, *263*, 39–47.
- [41] a) G. Hamasaka, T. Muto, Y. Uozumi, *Angew. Chem. Int. Ed.* **2011**, *50*, 4876–4878; *Angew. Chem.* **2011**, *123*, 4978–4980; b) G. Hamasaka, T. Muto, Y. Uozumi, *Dalton Trans.* **2011**, *40*, 8859–8868; c) G. Hamasaka, Y. Uozumi, *Chem. Lett.* **2016**, *45*, 1244–1246; d) G. Hamasaka, T. Muto, Y. Andoh, K. Fujimoto, K. Kato, M. Takata, S. Okazaki, Y. Uozumi, *Chem. Eur. J.* **2017**, *23*, 1291–1298; e) G. Hamasaka, Y. Uozumi, *Chem. Commun.* **2014**, *50*, 14516–14518.
- [42] A. Donner, K. Hagedorn, L. Mattes, M. Drechsler, S. Polarz, *Chem. Eur. J.* **2017**, *23*, 18129–18133.
- [43] A. C. Bijlard, S. Wald, D. Crespy, A. Taden, F. R. Wurm, K. Landfester, *Adv. Mater. Interfaces* **2017**, *4*, 1600443.
- [44] P. Brown, C. P. Butts, J. Eastoe, *Soft Matter* **2013**, *9*, 2365–2374.
- [45] X. F. Li, Y. Yang, J. Eastoe, J. F. Dong, *ChemPhysChem* **2010**, *11*, 3074–3077.
- [46] H. Y. Wang, B. Tan, J. J. Wang, Z. Y. Li, S. J. Zhang, *Langmuir* **2014**, *30*, 3971–3978.
- [47] Q. P. Duan, Y. Cao, Y. Li, X. Y. Hu, T. X. Xiao, C. Lin, Y. Pan, L. Y. Wang, *J. Am. Chem. Soc.* **2013**, *135*, 10542–10549.
- [48] M. Kishimoto, K. Kondo, M. Akita, M. Yoshizawa, *Chem. Commun.* **2017**, *53*, 1425–1428.
- [49] Y. X. Liu, P. G. Jessop, M. Cunningham, C. A. Eckert, C. L. Liotta, *Science* **2006**, *313*, 958–960.
- [50] Q. Zhang, G. Q. Yu, W. J. Wang, B. G. Li, S. P. Zhu, *Macromol. Rapid Commun.* **2012**, *33*, 916–921.
- [51] a) S. Polarz, S. Landsmann, A. Klaiiber, *Angew. Chem. Int. Ed.* **2014**, *53*, 946–954; *Angew. Chem.* **2014**, *126*, 962–970; b) S. Landsmann, C. Lizandara-Pueyo, S. Polarz, *J. Am. Chem. Soc.* **2010**, *132*, 5315–5321.
- [52] A. Klaiiber, C. Lanz, S. Landsmann, J. Gehring, M. Drechsler, S. Polarz, *Langmuir* **2016**, *32*, 10920–10927.
- [53] L. Zhao, S. Hao, Q. Zhai, H. Guo, B. Xu, H. Fan, *Soft Matter* **2017**, *13*, 3099–3106.
- [54] a) M. Subramanian, S. K. Mandal, S. Bhattacharya, *Langmuir* **1997**, *13*, 153–160; b) M. A. Susan, M. Begum, Y. Takeoka, M. Watanabe, *Langmuir* **2000**, *16*, 3509–3516.
- [55] T. Saji, K. Hoshino, S. Aoyagui, *Chem. Commun.* **1985**, 865–866.
- [56] a) P. Anton, J. Heinze, A. Laschewsky, *Langmuir* **1993**, *9*, 77–85; b) N. Aydogan, N. L. Abbott, *Langmuir* **2001**, *17*, 5703–5706; c) N. Aydogan, N. Aldis, *Langmuir* **2006**, *22*, 2028–2033.
- [57] X. Y. Liu, N. L. Abbott, *J. Colloid Interface Sci.* **2009**, *339*, 1–18.
- [58] Y. Chang, K. Yang, P. Wei, S. Huang, Y. Pei, W. Zhao, Z. Pei, *Angew. Chem. Int. Ed.* **2014**, *53*, 13126–13130; *Angew. Chem.* **2014**, *126*, 13342–13346.
- [59] a) J.-C. Eloi, D. A. Rider, G. Cambridge, G. R. Whittell, M. A. Winnik, I. Manners, *J. Am. Chem. Soc.* **2011**, *133*, 8903–8913; b) L. Liu, L. Rui, Y. Gao, W. Zhang, *Polym. Chem.* **2015**, *6*, 1817–1829; c) A. Feng, Q. Yan, H. Zhang, L. Peng, J. Yuan, *Chem. Commun.* **2014**, *50*, 4740–4742.
- [60] J. Li, M. Huo, J. Wang, J. Zhou, J. M. Mohammad, Y. Zhang, Q. Zhu, A. Y. Waddad, Q. Zhang, *Biomaterials* **2012**, *33*, 2310–2320.
- [61] J. E. Spallholz, *Free Radical Biol. Med.* **1994**, *17*, 45–64.
- [62] a) W. Kong, S. Guo, S. Wu, X. Liu, Y. Zhang, *Langmuir* **2016**, *32*, 9846–9853; b) Y. Zhang, W. Kong, C. Wang, P. An, Y. Fang, Y. Feng, Z. Qin, X. Liu, *Soft Matter* **2015**, *11*, 7469–7473.
- [63] a) J. Zhang, Y. F. Song, L. Cronin, T. B. Liu, *J. Am. Chem. Soc.* **2008**, *130*, 14408; b) P. C. Yin, D. Li, T. B. Liu, *Chem. Soc. Rev.* **2012**, *41*, 7368–7383; c) S. Polarz, J. A. Odendal, S. Hermann, A. Klaiiber, *Curr. Opin. Colloid Interface Sci.* **2015**, *20*, 151–160.
- [64] S. Landsmann, M. Wessig, M. Schmid, H. Colfen, S. Polarz, *Angew. Chem. Int. Ed.* **2012**, *51*, 5995–5999; *Angew. Chem.* **2012**, *124*, 6097–6101.
- [65] a) A. Klaiiber, S. Polarz, *ACS Nano* **2016**, *10*, 10041–10048; b) A. Klaiiber, T. Kollek, S. Cardinal, N. Hug, M. Drechsler, S. Polarz, *Adv. Mater. Interfaces* **2018**, *5*, 1701430.
- [66] J. M. Cases, F. Villieras, *Langmuir* **1992**, *8*, 1251–1264.
- [67] a) W. L. Hinze, E. Pramauro, *Crit. Rev. Anal. Chem.* **1993**, *24*, 133–177; b) H. Kunieda, K. Shinoda, *J. Dispersion Sci. Technol.* **1982**, *3*, 233–244.
- [68] a) D. Roy, W. L. A. Brooks, B. S. Sumerlin, *Chem. Soc. Rev.* **2013**, *42*, 7214–7243; b) A. Klaiherd, C. Nagamani, S. Thayumanavan, *J. Am. Chem. Soc.* **2009**, *131*, 4830–4838.
- [69] a) S. Qin, Y. Geng, D. E. Discher, S. Yang, *Adv. Mater.* **2006**, *18*, 2905–2909; b) J. Weiss, A. Laschewsky, *Langmuir* **2011**, *27*, 4465–4473; c) H.-i. Lee, J. A. Lee, Z. Poon, P. T. Hammond, *Chem. Commun.* **2008**, 3726–3728; d) Z. Zhu, N. Gao, H. Wang, S. A. Sukhishvili, *J. Controlled Release* **2013**, *171*, 73–80; e) C. Pietsch, U. Mansfeld, C. Guerrero-Sanchez, S. Hoepfener, A. Vollrath, M. Wagner, R. Hoogenboom, S. Saubern, S. H. Thang, C. R. Becer, *Macromolecules* **2012**, *45*, 9292–9302; f) V. Hildebrand, M. Heydenreich, A. Laschewsky, H. M. Möller, P. Müller-Buschbaum, C. M. Papadakis, D. Schanzbach, E. Wischerhoff, *Polymer* **2017**, *122*, 347–357.
- [70] J. K. Kim, E. Lee, Y. B. Lim, M. Lee, *Angew. Chem. Int. Ed.* **2008**, *47*, 4662–4666; *Angew. Chem.* **2008**, *120*, 4740–4744.
- [71] E. R. Kay, D. A. Leigh, F. Zerbetto, *Angew. Chem. Int. Ed.* **2007**, *46*, 72–191; *Angew. Chem.* **2007**, *119*, 72–196.
- [72] T. G. Shang, K. A. Smith, T. A. Hatton, *Langmuir* **2003**, *19*, 10764–10773.
- [73] S. S. Song, A. X. Song, J. C. Hao, *RSC Adv.* **2014**, *4*, 41864–41875.
- [74] a) S. Shinkai, K. Matsuo, A. Hagara, O. Manabe, *Perkin Trans. 2* **1982**, 1261–1265; b) S. Shinkai, K. Matsuo, M. Sato, T. Sone, O. Manabe, *Tetrahedron Lett.* **1981**, *22*, 1409–1412.
- [75] a) C. T. Lee, K. A. Smith, T. A. Hatton, *Macromolecules* **2004**, *37*, 5397–5405; b) H. Sakai, A. Matsumura, S. Yokoyama, T. Saji, M. Abe, *J. Phys. Chem. B* **1999**, *103*, 10737–10740; c) J. Y. Shin, N. L. Abbott, *Langmuir* **1999**, *15*, 4404–4410.
- [76] S. H. Peng, Q. P. Guo, T. C. Hughes, P. G. Hartley, *Langmuir* **2014**, *30*, 866–872.
- [77] Y. P. Wang, N. Ma, Z. Q. Wang, X. Zhang, *Angew. Chem. Int. Ed.* **2007**, *46*, 2823–2826; *Angew. Chem.* **2007**, *119*, 2881–2884.
- [78] a) H. I. Lee, W. Wu, J. K. Oh, L. Mueller, G. Sherwood, L. Peteanu, T. Kowalewski, K. Matyjaszewski, *Angew. Chem. Int. Ed.* **2007**, *46*, 2453–2457; *Angew. Chem.* **2007**, *119*, 2505–2509; b) Y. Ohya, Y. Okuyama, A. Fukunaga, T. Ouchi, *Supramol. Sci.* **1998**, *5*, 21–29; c) S. Samanta, J. Locklin, *Langmuir* **2008**, *24*, 9558–9565; d) A. Miyata, Y. Unuma, Y. Higashigaki, *Bull. Chem. Soc. Jap.* **1991**, *64*, 1719–1725; e) E. Ando, J. Miyazaki, K. Morimoto, H. Nakahara, K. Fukuda, *Thin Solid Films* **1985**, *133*, 21–28; f) D. A. Holden, H. Ringsdorf, V. Deblauwe, G. Smets, *J. Phys. Chem.* **1984**, *88*, 716–720.
- [79] A. L. Fameau, A. Arnould, M. Lehmann, R. von Klitzing, *Chem. Commun.* **2015**, *51*, 2907–2910.
- [80] a) D. H. W. Hubert, P. A. Cirkel, M. Jung, G. J. M. Koper, J. Meuldijk, A. L. German, *Langmuir* **1999**, *15*, 8849–8855; b) T. Shimomura, K. Ito, *Colloids Surf. A* **2002**, *209*, 281–287.
- [81] a) R. Dimova, K. A. Riske, S. Aranda, N. Bezlyepkina, R. L. Knorr, R. Lipowsky, *Soft Matter* **2007**, *3*, 817–827; b) D. L. Perrier, L. Rems, P. E. Boukany, *Adv. Colloid Interface Sci.* **2017**, *249*, 248–271; c) T. Portet, C. Mauroy, V. Démyer, T. Houles, J.-M. Escoffre, D. S. Dean, M.-P. Rols, *J. Membr. Biol.* **2012**, *245*, 555–564.
- [82] P. F. Salipante, P. M. Vlahovska, *Soft Matter* **2014**, *10*, 3386–3393.
- [83] A. K. Majhi, S. Kanchi, V. Venkataraman, K. G. Ayappa, P. K. Maiti, *Soft Matter* **2015**, *11*, 8632–8640.
- [84] A. A. Gurtovenko, A. S. Lyulina, *J. Phys. Chem. B* **2014**, *118*, 9909–9918.
- [85] a) C. K. Haluska, K. A. Riske, V. Marchi-Artzner, J.-M. Lehn, R. Lipowsky, R. Dimova, *Proc. Natl. Acad. Sci. USA* **2006**, *103*, 15841–15846; b) D. Raz-Ben Aroush, S. Yehudai-Resheff, K. Keren, *Methods Cell Biol.* **2015**, *125C*, 409–422.
- [86] J. M. Rabel, V. Aoun, I. Elkin, M. Mokhtar, P. Hildgen, *Curr. Med. Chem.* **2012**, *19*, 3070–3102.
- [87] J. T. Schwalbe, P. M. Vlahovska, M. J. Miksis, *Phys. Rev. E* **2011**, *83*, 046309.
- [88] K. A. Riske, R. Dimova, *Biophys. J.* **2006**, *91*, 1778–1786.
- [89] L. C. McConnell, P. M. Vlahovska, M. J. Miksis, *Soft Matter* **2015**, *11*, 4840–4846.
- [90] T. Yamamoto, S. Aranda-Espinoza, R. Dimova, R. Lipowsky, *Langmuir* **2010**, *26*, 12390–12407.

- [91] a) P. P. Borbat, A. J. Costa-Filho, K. A. Earle, J. K. Moscicki, J. H. Freed, *Science* **2001**, *291*, 266–269; b) C. L. Hawkins, M. J. Davies, *Biochim. Biophys. Acta Gen. Subj.* **2014**, *1840*, 708–721.
- [92] R. A. Sheldon, I. Arends, *Adv. Synth. Catal.* **2004**, *346*, 1051–1071.
- [93] K. Binnemans, C. Gorller-Walrand, *Chem. Rev.* **2002**, *102*, 2303–2345.
- [94] a) P. Brown, A. Bushmelev, C. P. Butts, J. Cheng, J. Eastoe, I. Grillo, R. K. Heenan, A. M. Schmidt, *Angew. Chem. Int. Ed.* **2012**, *51*, 2414–2416; *Angew. Chem.* **2012**, *124*, 2464–2466; b) P. Brown, C. P. Butts, J. Cheng, J. Eastoe, C. A. Russell, G. N. Smith, *Soft Matter* **2012**, *8*, 7545–7546; c) P. Brown, A. Bushmelev, C. P. Butts, J. C. Eloi, I. Grillo, P. J. Baker, A. M. Schmidt, J. Eastoe, *Langmuir* **2013**, *29*, 3246–3251.
- [95] P. Brown, T. A. Hatton, J. Eastoe, *Curr. Opin. Colloid Interface Sci.* **2015**, *20*, 140–150.
- [96] a) S. Polarz, C. Bahrle, S. Landsmann, A. Klaiber, *Angew. Chem. Int. Ed.* **2013**, *52*, 13665–13670; *Angew. Chem.* **2013**, *125*, 13910–13915; b) S. Hermann, M. Wessig, D. Kollofrath, M. Gerigk, K. Hagedorn, J. A. Odenal, M. Hagner, M. Drechsler, P. Erler, M. Fonin, G. Maret, S. Polarz, *Angew. Chem. Int. Ed.* **2017**, *56*, 5475–5479; *Angew. Chem.* **2017**, *129*, 5567–5571.

---

Manuscript received: May 7, 2018

Accepted manuscript online: June 28, 2018

Version of record online: October 30, 2018

---